Ion-assisted rotor airflow for residual fine-dust release from photovoltaic glass: a mechanism-isolation validation roadmap

Ridha Azaiz

Abstract

Residual fine dust on photovoltaic (PV) cover glass, concentrating solar power (CSP) mirrors and related exposed optical surfaces can persist after loose material has been displaced by wind, brushing or airflow. This paper addresses a defined mechanism-isolation question: whether rotor- or fan-carried ion delivery produces a measurable increment in a predeclared residual-response metric relative to matched airflow-only treatment under the same airflow condition, standoff, exposure time and initial surface state.

This paper presents a mechanism-isolation validation roadmap rather than integrated-system performance data, field deployment data or unmanned aerial vehicle (UAV) product validation. AIr denotes airflow with ion-assisted release. The roadmap defines an ion-assisted rotor-airflow architecture, separates the proposed mechanism from adjacent ionised-air, electrohydrodynamic (EHD), electrodynamic-screen and attractor-electrode approaches, and specifies the first falsifiable matched-control experiment required before integrated-system, field or product-performance claims can be made.

The proposed configuration is distinct from airflow-only treatment, stationary ionised-air knives, close-proximity ionic-wind devices and electrostatic collection systems because ion delivery and rotor- or fan-induced mobilisation are co-located within the same treatment footprint. Dust fate and redeposition are treated as validation endpoints rather than assumed outcomes. Optional sensing, self-calibration and control layers are engineering extensions; the core physical question is whether ion delivery changes the residual fine-dust removal threshold under matched airflow.

Keywords: ion-assisted rotor airflow; mechanism isolation; photovoltaic soiling; CSP mirrors; fine dust adhesion; electrostatic adhesion; EHD; matched-control validation; UAV translation.

1. Introduction

1.1 Residual fine dust and the central test

Photovoltaic (PV) and concentrating solar power (CSP) surfaces lose optical and electrical performance when particulate matter accumulates on exposed glass and mirror surfaces, and the magnitude of soiling loss depends on dust properties, climate, water availability and the maintenance method [1]–[7].

The narrower maintenance problem addressed here is residual fine material that remains after wind, brushing, coarse airflow or partial cleaning has displaced larger or more weakly adhered particles. In that regime, adhesion, charge state, particle history and redeposition become central to whether a dry, non-contact treatment can mobilise the residual film [8]–[13].

Water scarcity and wastewater constraints motivate dry or low-water maintenance, particularly in arid PV and CSP settings. In this roadmap, the relevant comparison is mechanistic rather than operational: whether ion delivery within the same rotor- or fan-generated flow that supplies near-wall shear and transport alters the residual fine-dust response under matched aerodynamic conditions. The water and soiling literature motivates the application context; it does not answer that mechanism-isolation question [1-7].

The first decisive test is whether the same predeclared residual-response metric is larger under ionised airflow than under matched airflow-only treatment. In notation, the primary test is:

$$\Delta_{res,ionised} > \Delta_{res,airflow-only}$$

Here Δres is the normalised residual-response metric, and the subscripts “ionised” and “airflow-only” label the two matched arms.

A positive result would establish a geometry- and surface-state-specific residual-response increment for the ionised-airflow arm relative to the matched airflow-only arm. It would not by itself establish field performance or UAV feasibility; those claims require subsequent translation and field studies.

1.2 Contribution and evidence tier

The central contribution is a mechanism-isolation framework for testing whether ion delivery changes the residual fine-dust removal threshold under matched airflow. The paper contributes four bounded elements: a co-delivery architecture; an adhesion, charge, EHD and redeposition vocabulary for interpreting the first test; a staged validation programme with matched airflow-only control; and an evidence-tier separation between fixed-rig mechanism validation, UAV translation, field performance and product readiness. This evidence-tier separation keeps adjacent-art plausibility, fixed-rig mechanism response, UAV translation, field performance and product readiness in distinct interpretive categories. Adjacent literature can support physical plausibility, identify comparators and inform controls, but it cannot be used as AIr-specific performance evidence.

Likewise, validation controls, sensors and endpoint matrices are research tools; they are not product requirements, operating limits or required embodiments. Detailed comparator matrices, validation arms, notation summaries, statement-boundary matrices and per-run reporting templates remain in Supplementary Tables S1–S13. The roadmap defines the decisive first comparison, the required measurements and the interpretation of positive, null and ambiguous outcomes before the architecture is evaluated as a UAV or field system. The decisive increment is not absolute cleaning efficiency; it is the differential residual response under matched airflow. Absolute cleaning efficiency, energy per area, coverage rate, reliability and autonomy are later evidence tiers.

1.3 Paper organisation

Section 2 compresses the related physics and adjacent art into an evidence-tier taxonomy. Section 3 defines the architecture and shows where airflow, ion delivery, electrostatic adhesion modification, EHD forcing, polarity and redeposition are physically distinct. Section 4 gives organising equations and boundary assumptions. Section 5 defines surface-state regimes. Section 6 specifies the decisive validation programme. Section 7 treats UAV translation as a later engineering-transfer problem. Sections 8 and 9 state limitations and conclusions.

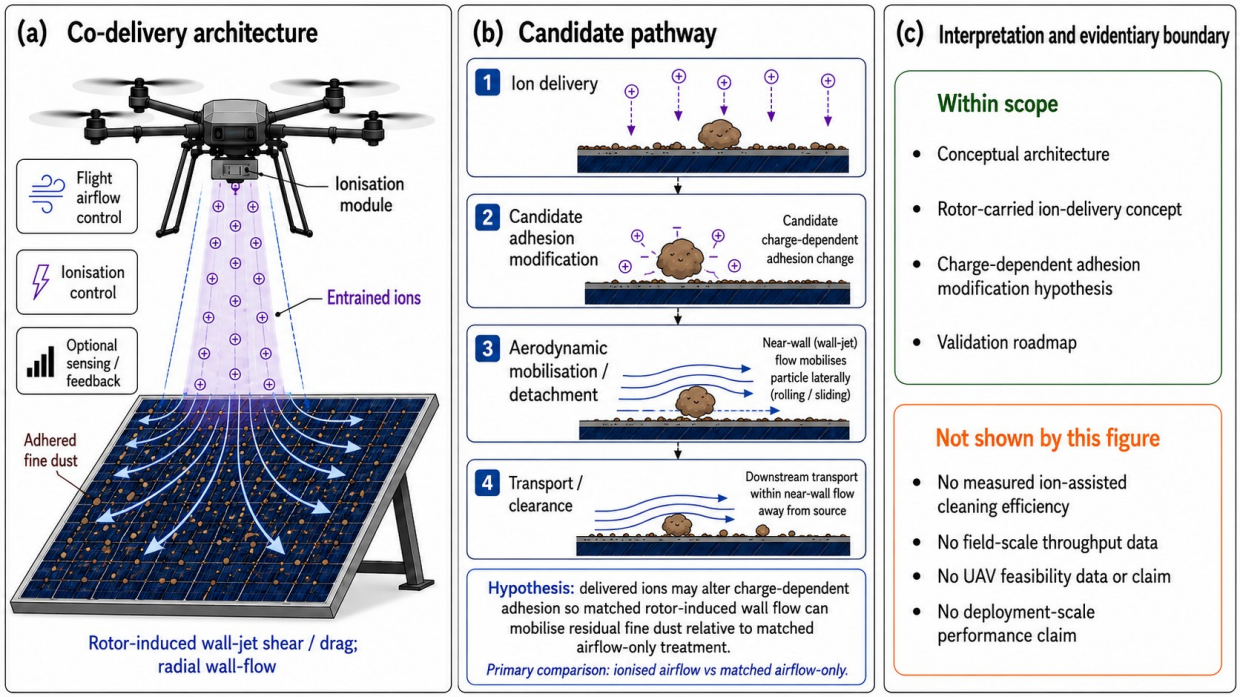

Figure 1. Conceptual ion-assisted rotor-airflow configuration, candidate pathway and evidentiary scope.

Panel (a) shows co-delivery of entrained ions and rotor-generated airflow toward a dust-loaded photovoltaic glass surface, followed by near-wall wall-jet transport. Panel (b) summarises the candidate pathway evaluated in this paper: ion delivery, possible charge- or contact-state response, and near-wall wall-jet mobilisation or possible clearance under matched rotor- or fan-generated airflow. The primary comparison remains ionised airflow versus matched airflow-only treatment; the pathway is a hypothesis, not a measured mechanism chain. Panel (c) defines the evidentiary boundary of the schematic; field throughput, field-scale feasibility, UAV feasibility and mechanism dominance are outside the present validation scope and require separate experiments.

2. Evidence Tier and Adjacent-Art Boundary

2.1 Adjacent-art context and evidentiary scope

The proposed architecture sits at the intersection of established but incomplete evidence streams: rotor and jet airflow physics [14-16], PV/CSP soiling studies, adhesion and electrostatic theory, stationary ionised-air PV comparisons, and close-proximity corona, EHD or ionic-wind cleaning studies. Representative sources from these groups motivate plausibility, terminology and control design within their respective geometries and evidence tiers.

The relevant boundary is architectural. Airflow-only approaches can mobilise particles by drag, shear, turbulent bursts, recirculation and wall flow. Stationary ionised-air knives can charge or neutralise particles in an externally supplied flow. Close-proximity EHD or ionic-wind systems can use electric body force and nearby return-path geometries [17]–[24]. Electrodynamic screens move particles using integrated electrodes [25]–[27].

Attractor-electrode systems can charge particles and collect or lift them toward a counter-electrode [13]. AIr, as framed here, instead tests whether ions carried by rotor or fan airflow change residual fine-dust removal under the same local flow that supplies mobilisation.

The evidence ladder is therefore: adjacent art establishes physical plausibility and comparator design; the first fixed-rig study can establish only a mechanism increment relative to matched airflow; UAV translation tests whether that increment can be carried into an aircraft-relevant footprint; field performance and product readiness remain separate later tiers. This hierarchy should be read together with Supplementary Tables S1, S6, S8 and S9. One public instantiation of the rotor-airflow cleaning architecture is documented in patent [40]. In this paper, experimental mechanism-validation evidence is reported separately from patent disclosures.

2.2 Strongest comparators and why they remain comparators

Al-Salaymeh et al. provide a PV-relevant stationary electrostatic/ionisation-based comparator rather than an AIr-equivalent architecture [28]. Its reported values are retained as adjacent-art context in Supplementary Table S1, not as expected AIr benchmarks.

Tilmatine, Kadous, Bendaoudi, Yanallah and related work provide close-proximity corona, EHD and ionic-wind comparators [18]–[22]. They are important because they demonstrate relevant electrostatic and ionic-wind physics, but their standoff, return-path, non-rotor-dominant or close-proximity geometries are not equivalent to rotor-entrained ion delivery. For that reason, the first AIr-specific comparison should be against matched airflow-only treatment, not against an unmatched adjacent device.

2.3 Reference strategy

References are used according to their evidentiary role in this roadmap. PV/CSP soiling literature motivates the application context; adhesion, electrostatic and rotor-flow literature provides mechanism vocabulary and validation variables; adjacent ionised-air, EHD and electrodynamic-screen studies inform comparator selection and control design; standards support measurement discipline; and patent documents identify public technical lineage and architecture provenance. AIr-specific residual-response increments, UAV translation and field performance are treated as later evidence tiers requiring matched-control testing. Reference-use and evidence-tier mapping is retained in Supplementary Tables S1 and S9 and the reference list.

This distinction is important because adjacent electrostatic, EHD and ionised-air studies are relevant to mechanism vocabulary and comparator design, but are not equivalent to the rotor-carried ion-delivery geometry considered here. A stationary ionised-air study can show that ion-loaded air can interact with dust on PV glass, while leaving rotor-plume ion delivery and matched near-wall shear to be tested separately. A close-proximity EHD study can show that space-charge body forces can move particles, while leaving rotor-dominant, EHD-assisted and coupled regimes to be separated in the proposed geometry. An attractor-electrode study can show a route for charged-particle collection, while the present non-collecting configuration requires dust-fate and redeposition measurements. These distinctions determine the controls needed for the first study. Comparator mechanisms, selected operating features and reported outcomes are summarised in Supplementary Table S1. The architectural implication is that none of those comparators removes the need for a matched airflow-only arm, panel-plane ion-dose measurement, redeposition mapping and polarity-aware interpretation.

3. Mechanism-Isolation Architecture

3.1 One treatment footprint, physically distinct functions

The architecture is framed as a co-delivery hypothesis rather than as a claim that ionisation replaces airflow. Rotor or fan airflow remains the mechanical mobilisation and transport field. Ion delivery is tested as a possible modifier of charge-sensitive adhesion, contact state, agglomerate cohesion, polarity-dependent Coulombic contribution or redeposition probability. EHD or ionic-wind forcing is a possible coupled contribution that must be measured or bounded rather than assumed negligible.

Two interpretation boundaries follow. First, airflow mobilisation does not require ions to move coarse or loosely adhered particles; the matched airflow-only arm defines this mechanical baseline and isolates any additional response attributable to ion delivery. Second, ion delivery alone is not claimed to remove dust; ioniser-on/motors-off or weak-flow conditions are mechanism controls, not product modes or substitutes for matched airflow. Charge can matter after initial motion as well as before it. A particle that is laterally displaced but remains close to the surface may re-adhere differently depending on its charge state, the local electric field, humidity and neighbouring particles. Redeposition maps should therefore be inspected for charge-dependent spatial patterns, not treated only as an operational nuisance.

Rotor or fan flow also has spatial and temporal structure. Blade-passage modulation, tip-vortex remnants, recirculation zones and wall-jet non-uniformity may modulate near-wall shear and removal or redeposition patterns, especially at close standoff. Removal and redeposition maps should therefore be checked for annular, streaked or blade-frequency-correlated structure so that rotor-flow signatures are not confused with ion-only or air-knife signatures.

3.2 Functional sequence

A default mechanism-isolation pass has four functions: create a repeatable near-surface flow; deliver ions into the same treatment footprint; expose a preconditioned residual fine-dust surface for a controlled dwell time; and measure residual response, redeposition and charge state with the same method in all arms. The essential measurement is not emitter output alone but panel-plane overlap between useful shear and useful ion dose. Emitter voltage describes the source; panel-plane ion flux is the measurement target. Optional sensors, feedback and calibration routines can improve repeatability, but they are not the core scientific claim. An open-loop fixed-rig implementation can be sufficient for the first falsifiable study if airflow, standoff, delivered ion proxy, surface state, exposure time and imaging geometry are controlled and reported.

The distinction between source settings and panel-plane conditions is central. Rotor speed, emitter voltage, electrode spacing and nominal standoff are not themselves mechanism variables unless they are translated into near-surface airflow, delivered ion current or dose, charge state and treatment footprint. A configuration that produces high ion output at the emitter but poor delivery at the panel plane is a negative or under-delivered mechanism test, not evidence against electrostatic adhesion modification in general. Conversely, a positive residual response without panel-plane measurements is weaker than a positive residual response accompanied by overlap between useful shear and delivered ion dose.

The same principle applies to dust fate. A cleared central region accompanied by charged redeposition, edge trapping or downstream accumulation may indicate particle redistribution rather than net residual-film reduction. The first study should therefore treat target-zone residual response and off-target deposition as paired outcomes. This is especially important for a non-collecting architecture, because the particle is not assumed to disappear from the module environment merely because it leaves the initial region of interest.

3.3 Control modes versus operating claims

The validation programme may include airflow-only, ionised airflow, ioniser-on/motors-off weak-flow/EHD-permitted exposure, sham geometry, stationary ionised-air positive control, polarity arms and system-charge audit conditions. These modes support mechanism attribution, identify coupled contributions and define boundary conditions. They are validation-protocol tools rather than product requirements, commercial modes, required embodiments or field-operating limits. Functional architecture modes and model-term definitions are expanded in Supplementary Tables S2 and S3; the minimum control set is expanded in Tables S6, S7 and S11.

4. Organising Physical Model

4.1 Adhesion limits and smooth-sphere vocabulary

The model is interpretive, not predictive. Johnson–Kendall–Roberts (JKR) and Derjaguin–Muller–Toporov (DMT) pull-off expressions provide limiting vocabulary for smooth elastic spheres; they are not quantitative predictions for irregular mineral dust on rough, contaminated PV glass. Real residual dust has shape, roughness, chemistry, humidity history and electrostatic state that are not captured by these smooth-sphere limits [29]–[33].

$$F_{pull,JKR} = \frac{3}{2}\pi R W \tag{1}$$

$$F_{pull,DMT} = 2\pi R W \tag{2}$$

Here R is particle radius and W is the work of adhesion in the idealised contact model. The equations are retained because they define how adhesion scales conceptually with size and interfacial energy, not because they predict AIr removal. Ion delivery need not create full normal lift-off to matter; a reduced rolling or sliding threshold can be sufficient if the matched airflow already supplies near-threshold lateral mobilisation. Conversely, any agglomerate-weakening interpretation requires pre/post microscopy or particle-size evidence and should not be inferred from the force model alone.

4.2 Threshold-crossing notation

The first mechanism hypothesis is that ion delivery can reduce an adhesion-resistance term enough for the same aerodynamic forcing to exceed the relevant residual-removal threshold. The organising inequalities are:

$$A_{flow} < R_{adh,0} \tag{3}$$

$$A_{flow} \geq R_{adh,ion} \tag{4}$$

$$\Delta R_{adh} = R_{adh,0} - R_{adh,ion} > 0 \tag{5}$$

$$R_{adh,after} \approx R_{adh,before} - \Delta R_{adh} \tag{6}$$

Here A_{flow} and R_{adh} are not universal force constants. They denote comparable, test-specific threshold quantities, such as force, stress, measured mobilisation threshold or nondimensional mobility index. The same definition and units, or the same nondimensionalisation, must be used consistently for the matched airflow-only and ionised-airflow arms.

The aerodynamic mobilisation term is not a universal shear or drag constant; it is a test-specific proxy. The baseline and ion-exposed adhesion-resistance terms are interpretive resistance terms before and after ion exposure. The equations should be read as a bookkeeping language for matched-control validation, not as a performance model.

In the schematics, the mobilising aerodynamic contribution is represented primarily as a surface-tangential wall-jet drag/shear term acting on rolling or sliding thresholds; any normal impingement or stagnation-pressure load is treated separately and should not be interpreted as the drag term responsible for mobilisation.

The resistance budget can include van der Waals attraction, image-charge/electrostatic terms, capillary bridges, chemical or salt-mediated binding, mechanical asperity pinning, agglomerate cohesion and re-adhesion tendency. The inferred adhesion-resistance change may reflect any combination of altered particle charge, image-charge attraction, rolling threshold, sliding threshold, contact pinning, cohesion or re-adhesion probability. The first study should not assign that change to a single sub-term unless diagnostic evidence supports that assignment. Van der Waals adhesion persists regardless of charge state; it is not directly ion-neutralisable.

This notation deliberately avoids an absolute removal prediction. The relevant threshold may be rolling, sliding, detachment, agglomerate break-up, or reduced probability of re-adhesion after a near-wall displacement. Those possibilities have different physical meanings and different diagnostic signatures. For example, a response dominated by agglomerate weakening should be accompanied by particle-size or microscopy evidence; a response dominated by charge neutralisation should be accompanied by charge-state change; a response dominated by EHD forcing should appear in high-voltage-on weak-flow or standoff-sweep controls. The notation is therefore a decision aid for experiment design, not a substitute for experiment.

The aerodynamic term is also intentionally abstract. In a mature study it could be replaced or supplemented by a measured wall-shear proxy, near-surface velocity statistic, turbulent-burst indicator, local pressure-gradient measure or calibrated particle-mobility surrogate. At the roadmap stage, forcing it into a single universal shear value would be misleading because rotor or fan flows near a finite surface can include impingement, radial wall jets, recirculation, blade-passage modulation and edge effects.

4.3 Electrostatic and polarity boundary

Image-charge scaling that depends on q_p^2 is an idealised conductor-plane approximation [34]. A PV module presents a multilayer dielectric/electrical boundary beneath and around the cover glass, including coatings, glass, encapsulant, cells, frames and possible moisture films; the conductor-plane expression is therefore only a warning that charge-sensitive adhesion can scale nonlinearly, not a literal surface model. Permittivity contrast and charge-relaxation timescale should be measured or bounded for the actual module stack rather than assumed from an ideal conductor limit. Polarity claims must remain conditional because unipolar ion delivery can either reduce or increase adhesion depending on particle sign, surface potential, field geometry, water films and deposition pathway.

Bipolar operation is best treated as a candidate neutralisation strategy for mixed or unknown charge distributions. Positive and negative unipolar modes are diagnostic polarity arms. A favourable unipolar response would support polarity-dependent mechanism under the tested condition; an unfavourable response could indicate Coulombic attraction, charge accumulation, wrong sign, poor field geometry or water-mediated screening.

For this reason, the appropriate first claim is not simply that ions reduce adhesion. The effect of ion delivery on adhesion depends on particle charge sign, surface potential, field geometry and water availability; a polarity-resolved, matched-airflow experiment is required to confirm a net favourable response under the intended surface state. Charge-sign assumptions should also be treated cautiously because contact electrification and granular deposition can generate size- and history-dependent charge states [35], [36].

Accordingly, Fes and any Coulombic contribution in the figure are sign- and boundary-condition-dependent terms, not fixed-direction forces.

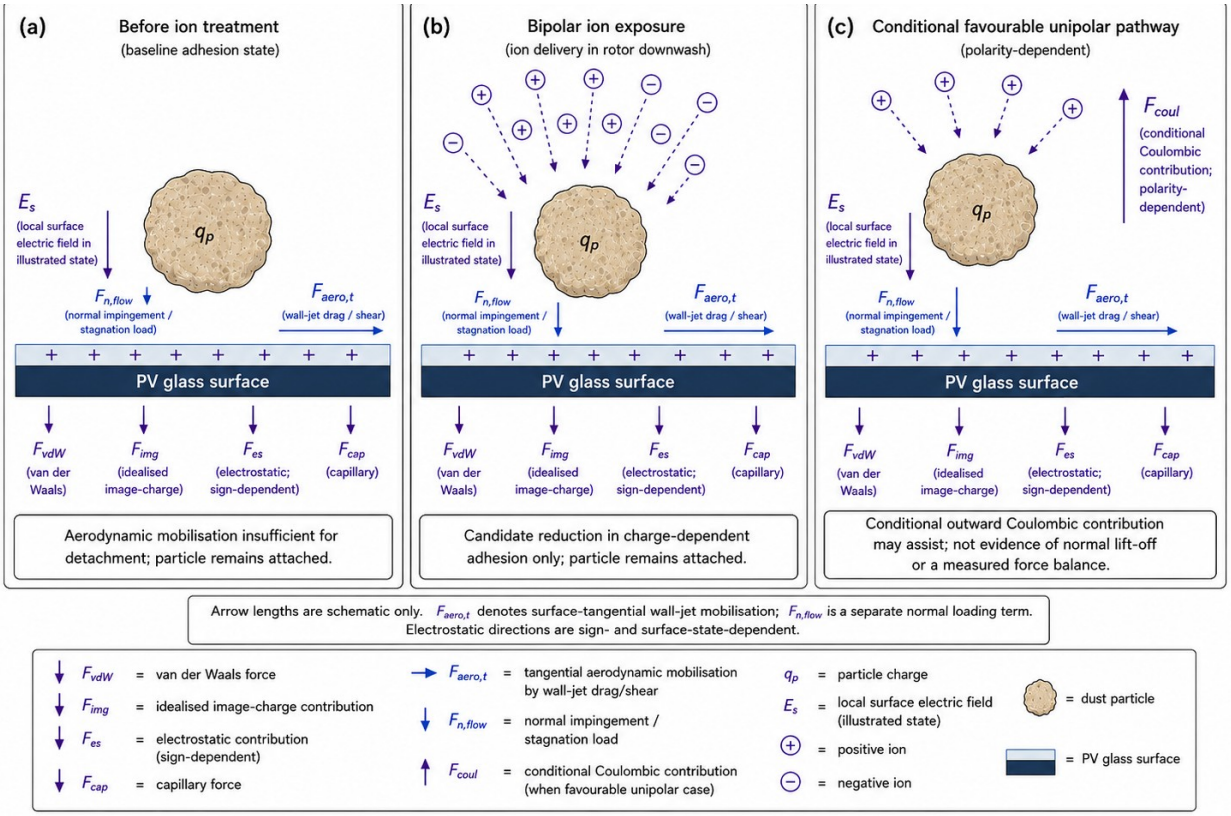

Figure 2. Particle-level force and charge model.

Arrow lengths are illustrative; force magnitudes are not quantified in this study. The schematic distinguishes surface-tangential aerodynamic mobilisation by near-wall wall-jet drag/shear, represented by Faero,t, from any surface-normal impingement or stagnation-pressure loading, represented by Fn,flow. Van der Waals, idealised image-charge, electrostatic and capillary terms are shown as adhesion or charge-sensitive contributions; their directions and magnitudes depend on particle charge, surface potential, humidity, contact state and boundary conditions. Panel (c) illustrates a conditional favourable unipolar pathway only; it is not evidence of pure normal lift-off or a measured force balance. The sign and magnitude of any ion-induced change remain hypotheses requiring matched-control measurement, not assumptions.

4.4 EHD and ion transport

EHD is not assumed secondary. Energised corona geometry can alter the local flow through space-charge body force, and that contribution may be coupled to rotor-induced shear near the surface. The useful question is not whether EHD exists, but whether it is negligible, co-primary or dominant in the tested geometry [17], [23], [24].

$$\Pi_{EHD} = \frac{\rho_q E}{\rho_{air} u_s^2 / L_c} \tag{7}$$

Here u_s denotes the selected near-surface velocity scale and L_c the selected comparison length. For fixed-rig comparisons, a defensible u_s choice could be a measured near-surface wall-jet peak velocity or a predeclared near-surface velocity statistic at the panel plane; it should not be replaced by rotor command, tip speed or emitter setting unless those quantities are calibrated to the panel-plane flow. The comparison in Eq. (7) is introduced here as a proposed comparison metric, not as a standard named EHD dimensionless group. It relates electric body-force density to a characteristic aerodynamic force-density scale. In that equation, the space-charge density, electric field, air density, selected near-surface velocity scale and selected comparison length are all geometry-specific quantities. The expression is a proposed organiser for comparing test configurations after geometry-specific calibration; it is not a predictive cleaning equation. The dimensionless and survival quantities in this section are triage metrics for regime classification - rotor-dominant, EHD-assisted, coupled, delivery-limited, dwell-limited or overlap-limited - not cleaning-efficiency predictors.

The same hardware may cross from rotor-dominant to EHD-dominant or coupled operation at reduced standoff. This EHD crossover standoff should be estimated experimentally by comparing polarity-resolved ion current, near-surface velocity or particle image velocimetry (PIV)/smoke response, and particle-removal response across standoff sweeps with high voltage on and off. The comparison length in Eq. (7) should be selected and reported as the same near-surface scale across the sweep, with sensitivity to reasonable choices stated rather than hidden in a universal value.

Ion transport to the panel plane is also a measurement problem. For a transport distance L and characteristic downwash velocity u_d, the transit time is:

$$t_{tr} = L / u_d \tag{8}$$

The estimate ttr = L/ud is a mean transit-time scale under a plug-flow approximation; turbulent rotor/fan flow will produce a distribution of arrival times rather than a single residence time.

For bipolar or mixed-polarity plumes, a simple ion-ion recombination survival scale is:

$$S_{rec} \approx \frac{1}{1 + \alpha\, n_0\, t_{tr}} \tag{9}$$

Here n0 denotes the initial small-ion concentration of either polarity under the balanced bipolar approximation, not the total positive-plus-negative ion concentration.

This expression assumes a balanced bipolar or mixed-polarity ion population represented by a lumped initial density, plug-flow transit over a characteristic time, and no spatial dilution, aerosol attachment or boundary interception unless those losses are separately included. It is therefore only an order-of-magnitude recombination warning, not a plume-resolved transport solution. This expression is not a generic unipolar loss law and should not be applied as one; unipolar operation requires separate treatment of space-charge drift, field geometry, aerosol attachment and boundary losses. A lumped first-order loss organiser can be written as Eq. (10).

$$S_{tot} \approx S_{rec} \exp\left[-\left(\beta_a N_a + k_{frame} + k_{wall} \right) t_{tr} \right] \tag{10}$$

In Eq. (10), βa is the aerosol-attachment coefficient [m^3 s^-1], Na is aerosol particle number concentration [m^-3], and kframe and kwall are lumped frame- and wall-loss rates [s^-1]. The Stot expression is introduced here only as a bookkeeping survival organiser for validation planning. It combines a standard bipolar recombination survival estimate with generic first-order sink terms for aerosol attachment and geometry-specific boundary interception. The terms kframe and kwall are not universal ion-transport constants; they are lumped loss rates to be measured, bounded or omitted according to the fixed-rig configuration. Equation (10) is not a plume-resolved transport solution and is not used to predict AIr cleaning performance.

The worked examples use a representative small-air-ion bipolar recombination coefficient near standard conditions, α ≈ 1.6 × 10^-12 m^3 s^-1, as an order-of-magnitude scale; reported values vary with ion composition, temperature, pressure and humidity [37], [38]. For example, at L = 0.3 m, ud = 3 m s^-1, and ttr ≈ 0.1 s, n0 = 10^15 m^-3 gives Srec ≈ 0.006, while n0 = 10^12 m^-3 gives Srec ≈ 0.86. A mid-scale value of n0 = 10^13 m^-3 gives an intermediate survival scale. The 10^15 m^-3 case should be read as a near-source or worst-case recombination illustration, not as a representative panel-plane delivered ion density. These are order-of-magnitude transport warnings, not predictions of dust removal; the panel-plane density, not the near-source output, is the relevant validation variable [37], [38].

The practical implication is that a validation report should not simply list emitter voltage or nominal ion concentration. It should record the delivery geometry, exposure distance, flow condition, polarity state, collector or probe location and any grounded or floating conductive boundaries that could intercept ions. Aerosol attachment, frame losses and wall losses may be negligible in some rigs and important in others; they should be bounded by measurement or stated as limitations. If the delivered ion dose cannot be measured directly, the study should use conservative proxy measurements and avoid strong mechanism attribution.

5. Surface-State Regimes and Boundary Conditions

5.1 Target regime

The primary validation target is residual fine mineral dust on dry or near-dry glass after loose material has been removed or standardised. The hypothesised advantage under very dry conditions is only a conditional adhesion-budget inference: if capillary bridges are weak and electrostatic/contact-state terms are important, ion delivery may matter. It is not a measured arid-site performance claim.

For the first validation campaign, the intended residual-fine-dust fraction should be predeclared by measured particle-size bins. An indicative core validation regime is micrometre-scale mineral dust, for example approximately 1-50 μm equivalent diameter, because this range is relevant to charge-sensitive adhesion and rolling/sliding-threshold interpretation. Coarser loose particles and submicrometre residues should be analysed separately rather than silently merged into the same endpoint.

5.2 Humidity, salts and cemented states

The intermediate humidity window is a validation hypothesis, not a characterised operating boundary. Dew, capillary bridges, salts, deliquescence, brine films, gypsum or cemented crusts, biofilms, oily contamination, snow, ice and wet mud may shift the limiting mechanism away from charge-sensitive fine-dust adhesion. These states require surface-state measurement rather than assumption from location, season or nominal relative humidity (RH). Boundary-regime logic is summarised in Supplementary Tables S4 and S5.

5.3 Electrical and charge persistence states

Electrical preconditioning, panel potential, frame grounding, dust charge and residual surface potential can alter interpretation. Charge persistence should be treated as a measured state variable. A positive ionised-airflow response without charge, ion-dose and surface-state records may be useful, but it is weaker mechanism evidence than a response accompanied by panel-plane ion delivery and charge-state measurements. Protocols should record pass-to-pass charge history rather than assuming every treatment begins from an identical electrical surface state. Surface chemistry should be recorded at the level needed for interpretation rather than as an exhaustive materials survey. Mineral dust, carbonaceous soot, pollen fragments, salts, gypsum-rich deposits and cemented mixtures can have different contact mechanics and different humidity responses. If the study uses a standardised surrogate dust, the surrogate should be described as a mechanism-screening material, not as a universal representation of field soiling. If naturally soiled coupons are used, the study should state how heterogeneity is blocked, randomised or imaged.

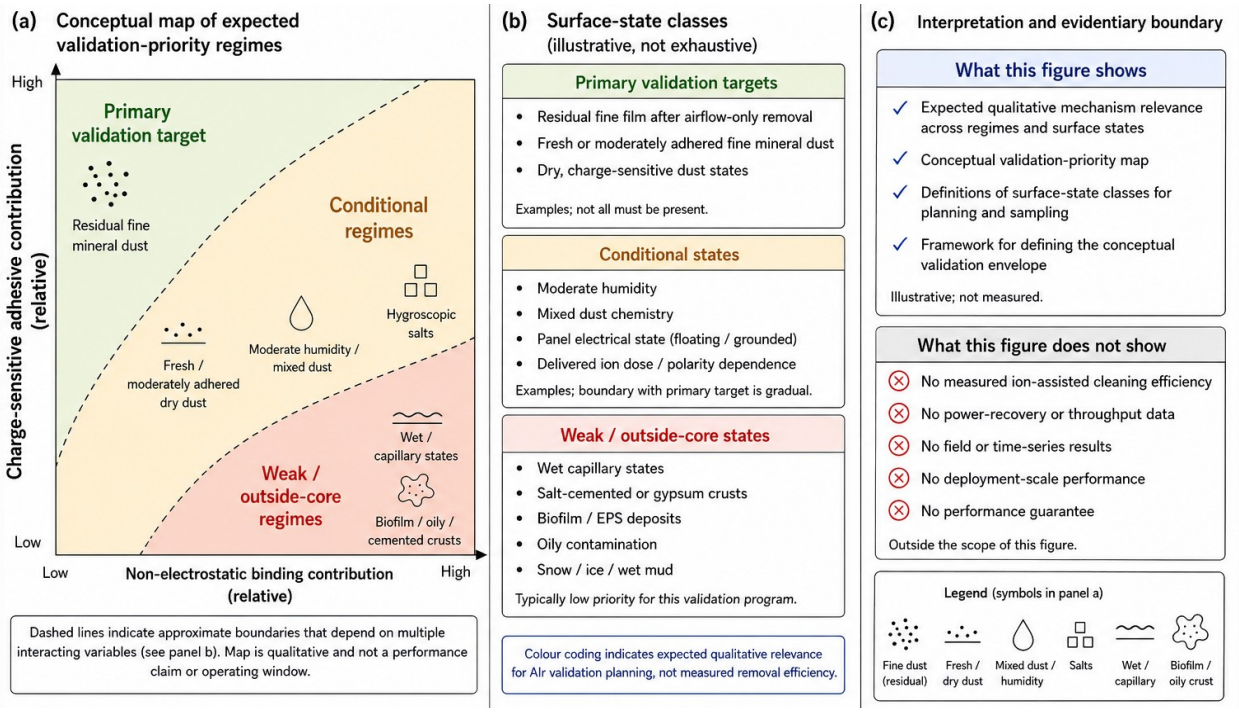

Figure 3. Conceptual operating-regime and surface-state map.

The map qualitatively organises expected validation priority for ion-assisted residual fine-dust mobilisation as a function of charge-sensitive adhesion contribution and non-electrostatic binding contribution. Primary validation targets include residual fine mineral dust after airflow-only removal and fresh or moderately adhered dry mineral dust. Conditional regimes include humidity, mixed dust chemistry, panel electrical state and delivered ion dose or polarity dependence. Weak or outside-core regimes include wet capillary states, salt-cemented or gypsum crusts, biofilm deposits, oily contamination, snow, ice and wet mud. Boundaries are illustrative and do not define measured operating windows, removal efficiencies or performance guarantees.

6. Experimental Validation Programme

6.1 Minimum decisive experiment

The minimum first study is a fixed-rig matched-control experiment. The same surface state, airflow proxy, standoff, exposure time, treatment footprint, imaging geometry and residual-response metric are used for two arms: matched airflow-only treatment and ionised airflow. The first decisive result is whether the ionised-airflow arm produces a larger residual-response increment than the matched airflow-only arm under the predeclared endpoint.

$$\Delta_{res,ionised} > \Delta_{res,airflow-only}$$

Here Δres is the normalised residual-response metric in the treatment region of interest, for example $(C_{baseline} - C_{post})/C_{baseline}$, where $C_{baseline}$ and C_{post} are the residual-film coverage, haze, attenuation, transmittance or equivalent optical/electrical proxy before and after treatment. The subscript baseline refers to the pre-treatment state for that specific arm and surface patch; post refers to the state after the controlled exposure.

6.2 Diagnostic extensions and core controls

Diagnostic controls should answer why the minimum test was positive, null or ambiguous. The minimum named set includes matched airflow-only, ionised airflow, ioniser-on/motors-off weak-flow/EHD-permitted exposure, sham ioniser geometry, and delivered-ion/charge audit conditions. Useful extensions include stationary ionised-air positive-control geometry, polarity arms, dust chemistry, humidity/dew-state logging, witness zones and redeposition mapping. These controls are research tools for mechanism attribution, not product requirements; the expanded control matrix and condensed validation checklist are provided in Supplementary Tables S6, S7, S11 and S12.

The sham-ioniser or sham-geometry control protects against attributing hardware-induced wake disturbance to ionisation. The ioniser-on/motors-off weak-flow/EHD-permitted arm protects against attributing EHD or corona flow effects to rotor-carried ion delivery. Matching must be done at the panel-plane airflow or shear proxy, not merely by using the same rotor command or emitter voltage. Full treatment matrices and per-run records are retained in Supplementary Tables S6, S7, S11 and S12. Minimum first-study reporting fields are summarised in Supplementary Table S13.

The first publishable study does not need every possible diagnostic branch to be successful, but it must be internally interpretable. At minimum, a reviewer should be able to see that the same endpoint was used for both arms, that the baseline surface state was comparable, that airflow matching was performed at the surface or through a reproducible proxy, that ion delivery was present at the panel plane, and that redeposition was not mistaken for removal. If these elements are missing, a positive visual difference would be difficult to separate from uncontrolled flow, lighting, initial dust heterogeneity or particle relocation.

Diagnostic extensions should be selected according to the most likely ambiguity. If the concern is EHD dominance, the high-voltage-on weak-flow arm and standoff sweep become important. If the concern is polarity, positive, negative and bipolar modes should be separated. If the concern is wet or salt-mediated adhesion, humidity, dew-point and surface chemistry logging become more important. If the concern is optical endpoint sensitivity, independent residual-film metrics should be compared. This targeted logic avoids presenting the full control matrix as a mandatory product recipe.

6.3 Redeposition, dust fate and spatial signatures

Because the proposed architecture does not intentionally collect particles, target-zone clearing cannot automatically be interpreted as net removal from the module environment. Witness zones around and downstream of the treatment footprint should be imaged so that re-adhesion, edge trapping and charge-dependent redeposition can be distinguished from true residual-film reduction. If redeposition concentrates in annular, streaked or blade-correlated patterns, the result should be interpreted as a coupled flow/charge outcome rather than a simple local-cleaning metric.

The endpoint hierarchy should therefore report at least three levels when possible: local residual response inside the treatment footprint, dust fate in surrounding witness zones, and any optical or electrical proxy that links residual film to functional surface performance. The first level is the most direct mechanism-isolation endpoint. The second protects against overstating target-zone clearing. The third may be useful for applied relevance, but it should not replace particle or film evidence in a first mechanism study.

6.4 Sampling, randomisation, safety and analysis

Test regions should be randomised and blocked across initial surface state, position and run order. Pilot planning can use 8 complete randomised blocks as a practical heuristic and 12–16 blocks as a starting point for a powered study, but formal power analysis should use pilot estimates of endpoint variance, intra-block correlation and the predeclared minimum detectable residual-film response. Sensitivity to endpoint choice should be reported rather than hidden.

Analysis should be framed around the paired or blocked contrast, not around post-hoc image selection. The primary contrast is the ionised-airflow residual response minus the matched airflow-only residual response for the predeclared endpoint and matched test condition. Secondary analyses can explore polarity, humidity, dust type, standoff or delivered dose, but these should be labelled exploratory unless powered and predeclared. Negative and ambiguous outcomes should be reported because they define the mechanism boundary and may be more informative than a visually favourable but poorly controlled pass.

If baseline residual coverage differs between matched arms after blocking or randomisation, the analysis should report baseline values and use a paired/block-normalised comparison or a baseline-adjusted model rather than comparing unadjusted post-treatment values alone.

Ozone and by-product safety should be treated as part of the validation protocol rather than as a later product topic. Representative duty cycles should include ozone monitoring, predeclared stop criteria and material-compatibility checks; if nitrogen oxides (NO_x), volatile organic compounds (VOCs) or aldehyde screening is unavailable, that limitation should be stated. International Electrotechnical Commission (IEC) ionisation test practice and occupational ozone references can guide measurement discipline without converting validation checks into product claims [10], [39]. Indoor bipolar-ionisation studies are cited only to motivate by-product monitoring discipline, not as PV-field or AIr-specific safety validation [11].

6.5 Outcome interpretation and progression logic

A positive response supports the mechanism only within the tested surface state, geometry and endpoint. A null response can be informative if ion dose, footprint overlap, wall shear and surface state were adequately measured; it may indicate insufficient delivered ion dose, wrong polarity, EHD contribution as an attribution risk, capillary/cemented adhesion, redeposition, poor overlap or insufficient airflow. An ambiguous response should redirect the validation programme rather than be reframed as performance evidence.

Progression beyond the first fixed-rig study should be conditional. The next study should be chosen according to the limiting uncertainty: delivered ion dose, polarity, EHD contribution, flow/ion overlap, redeposition, surface-state boundary or metric sensitivity. Cleaning efficiency, field throughput, energy per area, autonomy and field-readiness metrics belong to later evidence tiers after the mechanism-isolation increment has been tested.

Outcome interpretation should remain conservative. A positive outcome means that the ionised-airflow arm exceeded the matched airflow-only arm on the predeclared endpoint while ion delivery and surface state were adequately documented. A null outcome means that no additional residual response was detected under those conditions, not that ion-assisted mechanisms are impossible. An ambiguous outcome means that unresolved attribution factors, such as poor airflow matching, insufficient delivered dose, uncontrolled surface state, EHD dominance or redeposition, limit interpretation of the mechanism. This scheme keeps positive, null and ambiguous outcomes separately interpretable.

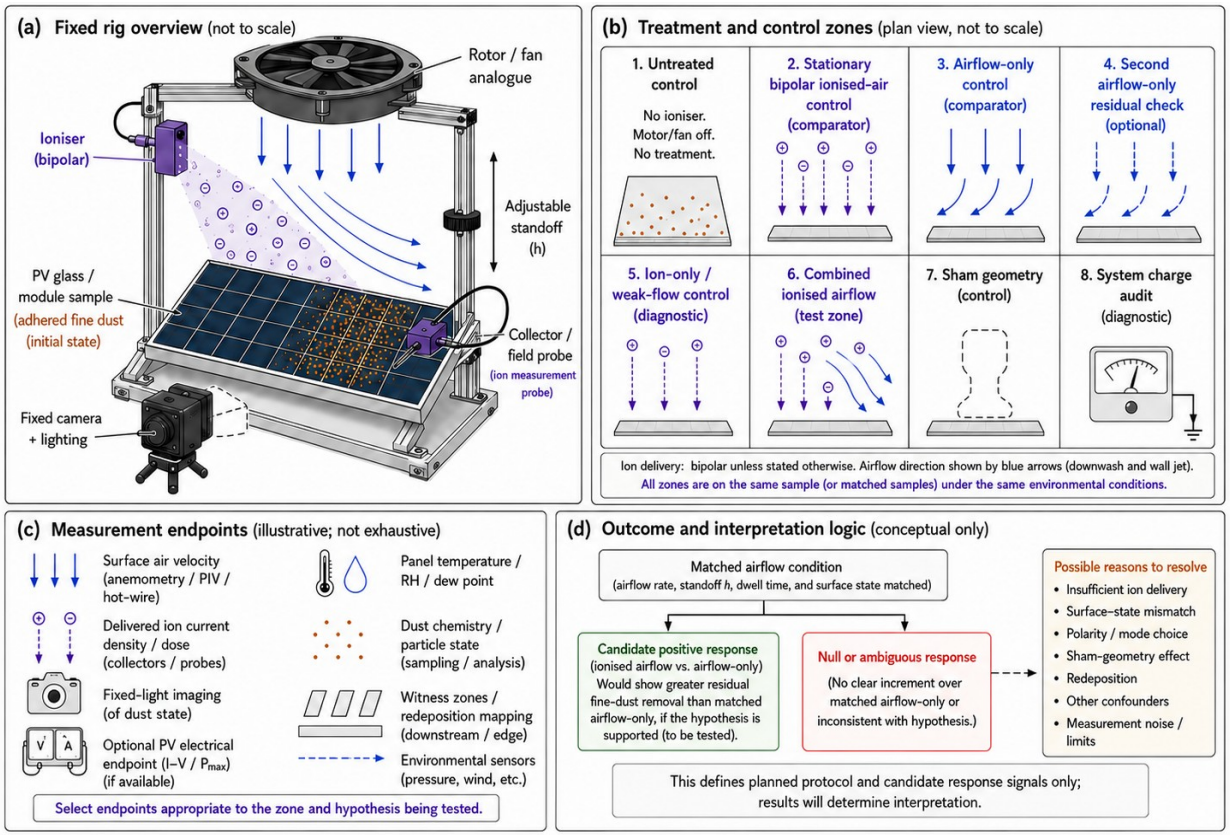

Figure 4. Proposed experimental validation protocol for mechanism-isolation planning.

Fixed-rig validation schematic showing a rotor/fan analogue, ion-delivery path, PV glass or module sample, panel-plane collector or field probe, fixed imaging geometry and matched treatment/control zones. Treatment arms distinguish untreated control, stationary bipolar ionised-air comparator, matched airflow-only control, optional second airflow-only residual check, ion-only or weak-flow diagnostic, combined ionised airflow, sham geometry and system-charge audit conditions. Measurement endpoints include surface air velocity, delivered ion current or dose, fixed-light imaging, optional PV electrical endpoint, temperature/relative humidity/dew-point state, dust chemistry, particle state, witness zones and redeposition mapping. Outcome boxes define candidate interpretation logic only; results will determine whether the hypothesis is supported, null or ambiguous.

7. UAV Translation Boundary

7.1 Translation question

UAV translation is an engineering-transfer problem, not an outcome of the fixed-rig mechanism test. The fixed-rig question is whether ionised airflow outperforms matched airflow-only under controlled conditions. The UAV question is whether useful ion dose and useful wall shear can overlap at the panel plane within acceptable standoff, dwell, mass, power, safety and control constraints.

The staged path should be fixed-rig mechanism validation first, then rotor-stand or tethered-platform translation, and only later free-flight or field testing. A fixed-rig mechanism increment is publishable as a validation result only within its tier; it is not a demonstration of airborne deployment.

At each stage the claim changes. A fixed rig can support mechanism isolation. A rotor stand can test whether useful ion dose and useful wall shear survive aircraft-relevant downwash, standoff and footprint constraints. A tethered or constrained platform can add positioning, vibration, attitude and dwell variation. A free-flight study can address coverage, autonomy, repeatability and operational safety. These stages should not be collapsed into a single field-readiness claim.

7.2 Surface-level variables

The relevant translation variables are effective swath width, standoff, traverse speed, dwell time, delivered ion dose, flow/ion footprint overlap, frame charge, high-voltage (HV) safety, electromagnetic interference and electromagnetic compatibility (EMI/EMC), ozone or by-product exposure, material compatibility, redeposition and coverage-rate/autonomy estimate. These are later measurement targets. They should not be converted into implied product specifications. The UAV transfer checklist remains in Supplementary Table S8.

7.3 Lightweight target

A sub-250 g aircraft remains a design target that requires a staged translation study. This paper addresses the mechanism-isolation tier; aircraft integration would require separate mass, power, shielding, control, safety and panel-plane ion/flow-overlap validation before lightweight UAV feasibility could be claimed.

This distinction also preserves the interpretation of a future prototype. If a lightweight platform meets a mass target but cannot deliver the required panel-plane ion/flow overlap, the mechanism has not transferred. If a heavier platform demonstrates the overlap cleanly, that result may still be scientifically valuable even if it does not meet the original aircraft-design target. Mass class is therefore an engineering constraint, not a substitute for mechanism evidence.

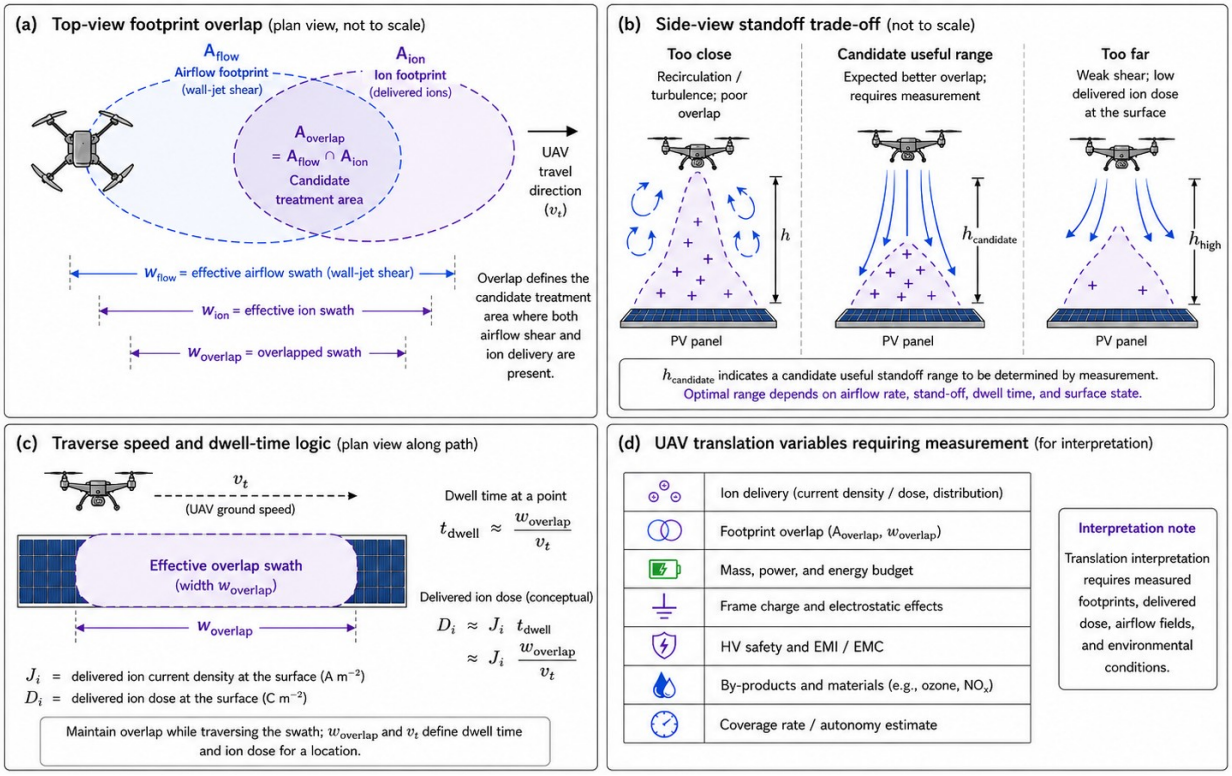

Figure 5. Airflow and ion-footprint overlap as a UAV translation concept.

Conceptual schematic of the translation variables that must be measured before field or deployment claims are made. Panel (a) defines the candidate treatment area as the overlap between the surface-flow footprint and delivered-ion footprint. Panel (b) illustrates the standoff trade-off between recirculation or poor overlap at very small standoff, a candidate standoff range to be determined by measurement, and weak shear or low delivered ion dose at excessive standoff; it does not define an optimised or validated operating window. Panel (c) shows dwell-time and delivered-dose scaling with effective overlap width and traverse speed as conceptual scaling relations, not cleaning-efficiency predictions. Panel (d) lists translation variables requiring measurement: ion delivery, footprint overlap, mass and power budget, frame charge and electrostatic effects, HV safety and EMI/EMC, by-products and materials, and coverage-rate/autonomy estimate.

8. Discussion

8.1 Defined Contributions of the Roadmap

The framework separates the first falsifiable mechanism-isolation test from later performance and deployment evidence. A fixed rig can test overlap between delivered ion dose and useful shear under controlled surface state; aircraft transfer, field throughput, energy per area and product reliability are addressed at later evidence tiers. A UAV translation study can test whether the mechanism survives aircraft-relevant standoff, swath width, mass, power and safety constraints; long-term field performance requires separate operational evidence.

8.2 Questions Reserved for Subsequent Validation

The architecture-specific performance increment remains to be quantified under matched-control conditions: useful ions must reach the dust/glass interface within the same treatment footprint as useful rotor- or fan-induced mobilisation, and that co-delivery must produce an additional residual fine-dust response beyond matched airflow-only treatment. This roadmap defines the first falsifiable test needed to quantify that increment within the mechanism-isolation framework.

The main interpretation risks are overinterpretation and under-instrumentation. The evidence hierarchy prevents adjacent-art plausibility from substituting for mechanism-isolation data: fixed-rig mechanism increment, UAV transfer, field performance and product readiness are separate evidence tiers, and the present work is limited to the mechanism-isolation tier. The validation programme reduces under-instrumentation by naming the minimum control arms, dose measurements, EHD checks, surface-state records and redeposition endpoints needed for an interpretable first result.

The evidence-tier structure prevents adjacent-art plausibility, fixed-rig response, UAV translation and field performance from being conflated. This structure keeps positive, null and ambiguous outcomes interpretable without treating validation controls as product requirements.

9. Conclusion

Here, ion-assisted rotor airflow is treated as a mechanism-isolation framework: ions carried by rotor or fan airflow may alter charge-sensitive adhesion, contact state, polarity-dependent force balance, agglomerate behaviour or redeposition probability sufficiently to produce a surface-state-specific residual-response increment beyond matched airflow-only treatment.

The initial validation step is to compare a predeclared residual-response metric under ionised airflow with the same metric under matched airflow-only treatment, using the same surface state, airflow condition, standoff, exposure time and endpoint definition. A positive result would support a surface-state- and geometry-specific mechanism increment. A null or ambiguous result would identify the next limiting uncertainty. Integrated-system cleaning performance, field deployment capability and UAV product readiness are addressed at later evidence tiers.

Accordingly, this paper provides a mechanism-isolation validation architecture rather than measured integrated-system performance. It defines the discriminating comparison, the variables that must be controlled, the measurements needed to preserve mechanism attribution, and the interpretation of positive, null and ambiguous outcomes. Such a result would justify UAV-translation and field-performance studies.

References

[1] IEA PVPS Task 13. Soiling Losses: Impact on the Performance of Photovoltaic Power Plants; Report IEA-PVPS T13-21:2022; International Energy Agency Photovoltaic Power Systems Programme: Paris, France, 2022.

[2] Maghami, M.R.; Hizam, H.; Gomes, C.; Radzi, M.A.; Rezadad, M.I.; Hajighorbani, S. Power loss due to soiling on solar panel: A review. Renew. Sustain. Energy Rev. 2016, 59, 1307-1316. https://doi.org/10.1016/j.rser.2016.01.044.

[3] Ilse, K.K.; Figgis, B.W.; Naumann, V.; Hagendorf, C.; Bagdahn, J. Fundamentals of soiling processes on photovoltaic modules. Renew. Sustain. Energy Rev. 2018, 98, 239-254. https://doi.org/10.1016/j.rser.2018.09.015.

[4] Wan, L.; Zhao, L.; Xu, W.; Guo, F.; Jiang, X. Dust deposition on the photovoltaic panel: A comprehensive survey on mechanisms, effects, mathematical modeling, cleaning methods, and monitoring systems. Sol. Energy 2024, 268, 112300. https://doi.org/10.1016/j.solener.2023.112300.

[5] Parsay, A.; Gandomzadeh, M.; Yaghoubi, A.A.; Hoorsun, A.; Gholami, A.; Zandi, M.; Gavagsaz-Ghoachani, R.; Kazem, H.A. Enhancing photovoltaic efficiency: An in-depth systematic review and critical analysis of dust monitoring, mitigation, and cleaning techniques. Appl. Energy 2025, 388, 125668. https://doi.org/10.1016/j.apenergy.2025.125668.

[6] Ouarzazate Solar Power Complex, Phase 1, Morocco: Specific Environmental and Social Impact Assessment, Volume 1; Official Project Environmental and Social Impact Assessment Report for Noor I/Ouarzazate Solar Power Station, 2012.

[7] Bracken, N.; Macknick, J.; Tovar-Hastings, A.; Komor, P.; Gerritsen, M.; Mehos, M. Concentrating Solar Power and Water Issues in the U.S. Southwest; Technical Report NREL/TP-6A50-61376; National Renewable Energy Laboratory: Golden, CO, USA, 2015.

[8] Rehman, S.; Mohandes, M.A.; Hussein, A.E.; Alhems, L.M.; Al-Shaikhi, A. Cleaning of photovoltaic panels utilizing the downward thrust of a drone. Energies 2022, 15, 8159. https://doi.org/10.3390/en15218159.

[9] Jiang, C.-S.; Moutinho, H.R.; To, B.; Xiao, C.; Simpson, L.J.; Al-Jassim, M.M. Long-lasting strong electrostatic attraction and adhesion forces of dust particles on photovoltaic modules. Sol. Energy Mater. Sol. Cells 2020, 204, 110206. https://doi.org/10.1016/j.solmat.2019.110206.

[10] International Electrotechnical Commission. IEC 61340-4-7:2025, Electrostatics - Part 4-7: Standard Test Methods for Specific Applications - Ionization, 3rd ed.; International Electrotechnical Commission: Geneva, Switzerland, 2025.

[11] Zeng, Y.; Manwatkar, P.; Laguerre, A.; Gunsch, M.J.; Heidarinejad, M.; Stephens, B. Evaluating a commercially available in-duct bipolar ionization device for pollutant removal and potential byproduct formation. Build. Environ. 2021, 195, 107750. https://doi.org/10.1016/j.buildenv.2021.107750.

[12] Kunkel, W.B. The static electrification of dust particles on dispersion into a cloud. J. Appl. Phys. 1950, 21, 820-832.

[13] Dust Cleaning and Collecting Device Based on Electrostatic Principles. WO Patent WO2010109261A1, 30 September 2010.

[14] Bauersfeld, L.; Muller, K.; Ziegler, D.; Coletti, F.; Scaramuzza, D. Robotics meets fluid dynamics: A characterization of the induced airflow below a quadrotor as a turbulent jet. IEEE Robot. Autom. Lett. 2025, 10, 1241-1248. https://doi.org/10.1109/LRA.2024.3518835.

[15] Leishman, J.G. Principles of Helicopter Aerodynamics; Cambridge University Press: Cambridge, UK, 2006.

[16] Metzger, J.P.; Mehring, C. Particle removal from solid surfaces via an impinging gas jet pulse: Comparison between experimental and CFD-DEM modeling results. J. Aerosol Sci. 2024, 179, 106364. https://doi.org/10.1016/j.jaerosci.2024.106364.

[17] Cobine, J.D. Gaseous Conductors: Theory and Engineering Applications; McGraw-Hill: New York, NY, USA, 1941.

[18] Tilmatine, A.; Kadous, N.; Yanallah, K.; Bellebna, Y.; Bendaoudi, Z.; Zouaghi, A. Experimental investigation of a new solar panels cleaning system using ionic wind produced by corona discharge. J. Electrostat. 2023, 124, 103827. https://doi.org/10.1016/j.elstat.2023.103827.

[19] Yanallah, K.; Bouazza, M.R.; Tilmatine, A.; Pontiga, F.; Zouaghi, A.; Kadous, N.; Bellebna, Y. Numerical modeling of dust particle motion in a corona discharge-based ionic wind cleaning system for solar panels. J. Electrostat. 2026, 140, 104262. https://doi.org/10.1016/j.elstat.2026.104262.

[20] Kadous, N.; Yanallah, K.; Bellebna, Y.; Bendaoudi, Z.; Tilmatine, A. Exploring the effectiveness of a novel cleaning method for solar panels using corona ionic wind. Part. Sci. Technol. 2024, 42, 324-330. https://doi.org/10.1080/02726351.2023.2243857.

[21] Bendaoudi, Z.; Namoune, A.; Kadous, N.; Bellebna, Y.; Yanallah, K.; Tilmatine, A. An improved electrostatic cleaning system for dust removal from photovoltaic panels. J. Eng. Sci. Technol. Rev. 2024, 17, 109-115. https://doi.org/10.25103/jestr.171.14.

[22] Yanallah, K.; Chelih, A.; Bellebna, Y.; Kadous, N.; Bendaoudi, Z.; Zouaghi, A.; Tilmatine, A.; Canale, L. Numerical analysis of a new corona ionic wind blower used for solar panel cleaning. IEEE Trans. Ind. Appl. 2025, 61, 3502-3511. https://doi.org/10.1109/TIA.2025.3531827.

[23] Moreau, E.; Audier, P.; Benard, N. Ionic wind produced by positive and negative corona discharges in air. J. Electrostat. 2018, 93, 85-96. https://doi.org/10.1016/j.elstat.2018.03.009.

[24] Castellanos, A. Basic concepts and equations in electrohydrodynamics. In Electrohydrodynamics; Castellanos, A., Ed.; Springer: Vienna, Austria, 1998.

[25] Kawamoto, H.; Shibata, T. Electrostatic cleaning system for removal of sand from solar panels. J. Electrostat. 2015, 73, 65-70. https://doi.org/10.1016/j.elstat.2014.10.011.

[26] Panat, S.; Varanasi, K.K. Electrostatic dust removal using adsorbed moisture-assisted charge induction for sustainable operation of solar panels. Sci. Adv. 2022, 8, eabm0078. https://doi.org/10.1126/sciadv.abm0078.

[27] Dickhardt, F.J.; Panat, S.; Varanasi, K.K. Enhanced electrostatic dust removal from solar panels using transparent conductive nano-textured surfaces. Small 2025, 21, 2408645. https://doi.org/10.1002/smll.202408645.

[28] Al-Salaymeh, A.S.; Al-Mansi, N.N.; Muslih, I.M.; Altaharwah, Y.A.; Al Smadi, W.Y. Electrostatic cleaning effect on the performance of PV modules in Jordan. Clean. Eng. Technol. 2023, 13, 100606. https://doi.org/10.1016/j.clet.2023.100606.

[29] Moutinho, H.R.; Jiang, C.-S.; To, B.; Perkins, C.; Muller, M.; Al-Jassim, M.; Simpson, L. Adhesion mechanisms on solar glass: Effects of relative humidity, surface roughness, and particle shape and size. Sol. Energy Mater. Sol. Cells 2017, 172, 145-153. https://doi.org/10.1016/j.solmat.2017.07.026.

[30] Yilbas, B.S.; Ali, H.; Khaled, M.M.; Al-Aqeeli, N.; Abu-Dheir, N.; Varanasi, K.K. Influence of dust and mud on the optical, chemical, and mechanical properties of a PV protective glass. Sci. Rep. 2015, 5, 15833. https://doi.org/10.1038/srep15833.

[31] Isaifan, R.J.; Johnson, D.; Ackermann, L.; Figgis, B.; Ayoub, M. Evaluation of the adhesion forces between dust particles and photovoltaic module surfaces. Sol. Energy Mater. Sol. Cells 2019, 191, 413-421. https://doi.org/10.1016/j.solmat.2018.11.031.

[32] Johnson, K.L.; Kendall, K.; Roberts, A.D. Surface energy and the contact of elastic solids. Proc. R. Soc. Lond. A 1971, 324, 301-313. https://doi.org/10.1098/rspa.1971.0141.

[33] Derjaguin, B.V.; Muller, V.M.; Toporov, Y.P. Effect of contact deformations on the adhesion of particles. J. Colloid Interface Sci. 1975, 53, 314-326. https://doi.org/10.1016/0021-9797(75)90018-1.

[34] Griffiths, D.J. Introduction to Electrodynamics, 4th ed.; Pearson: Boston, MA, USA, 2013.

[35] Lacks, D.J.; Sankaran, R.M. Contact electrification of insulating materials. J. Phys. D Appl. Phys. 2011, 44, 453001. https://doi.org/10.1088/0022-3727/44/45/453001.

[36] Kok, J.F.; Lacks, D.J. Electrification of granular systems of identical insulators. Phys. Rev. E 2009, 79, 051304. https://doi.org/10.1103/PhysRevE.79.051304.

[37] Wright, M.D.; Matthews, J.C.; Shallcross, D.E. A quasi-one-dimensional model for ion-aerosol interactions and aerosol charge state downwind of corona-producing alternating current (AC) HVPL under stable atmospheric conditions. Environ. Res. 2023, 231, 115908. https://doi.org/10.1016/j.envres.2023.115908.

[38] Harrison, R.G.; Carslaw, K.S. Ion-aerosol-cloud processes in the lower atmosphere. Rev. Geophys. 2003, 41, 1012. https://doi.org/10.1029/2002RG000114.

[39] National Institute for Occupational Safety and Health. Ozone. NIOSH Pocket Guide to Chemical Hazards; Centers for Disease Control and Prevention: Atlanta, GA, USA. Available online: https://www.cdc.gov/niosh/npg/npgd0476.html (accessed on 6 June 2026).

[40] Azaiz, R. Method for controlling a flying object for cleaning surfaces. U.S. Patent US10046857B2, 14 August 2018.